Published in final edited form as:
Neuroscience. 2009 December 15; 164(3): 1334–1346. doi:10.1016/j.neuroscience.2009.09.024.

Amyloid-β expression in retrosplenial cortex of 3xTg-AD mice: relationship to cholinergic axonal afferents from medial septum

Richard T. Robertson[1], **Janie Baratta**[1], **Jen Yu**[2], and **Frank M. LaFerla**[3]

[1] Department of Anatomy and Neurobiology, Institute for Memory Impairments and Neurological Disorders, University of California, Irvine, Irvine, CA 92697

[2] Department of Physical Medicine and Rehabilitation, Institute for Memory Impairments and Neurological Disorders, University of California, Irvine, Irvine, CA 92697

[3] Department of Neurobiology & Behavior, Institute for Memory Impairments and Neurological Disorders, University of California, Irvine, Irvine, CA 92697

Abstract

Triple transgenic (3xTg-AD) mice harboring the presenilin 1, amyloid precursor protein, and tau transgenes (Oddo et al., 2003) display prominent levels of amyloid-beta (Aβ) immunoreactivity in forebrain regions. The Aβ immunoreactivity is first seen intracellularly in neurons and later as extracellular plaque deposits. The present study examined Aβ immunoreactivity that occurs in layer III of the granular division of retrosplenial cortex (RSg). This pattern of Aβ immunoreactivity in layer III of RSg develops relatively late, and is seen in animals older than 14 mo. The appearance of the Aβ immunoreactivity is similar to an axonal terminal field and thus may offer a unique opportunity to study the relationship between afferent projections and the formation of Aβ deposits. Axonal tract tracing techniques demonstrated that the pattern of axon terminal labeling in layer III of RSg, following placement of DiI in medial septum, is remarkably similar to the pattern of cholinergic axons in RSg, as detected by acetylcholinesterase histochemical staining, choline acetyltransferase immunoreactivity, or p75 receptor immunoreactivity; this pattern also is strikingly similar to the band of Aβ immunoreactivity. In animals sustaining early damage to the medial septal nucleus (prior to the advent of Aβ immunoreactivity), the band of Aβ in layer III of RSg does not develop; the corresponding band of cholinergic markers also is eliminated. In older animals (after the appearance of the Aβ immunoreactivity) damage to cholinergic afferents by electrolytic lesions, immunotoxin lesions, or cutting the cingulate bundle, result in a rapid loss of the cholinergic markers and a slower reduction of Aβ immunoreactivity. These results suggest that the septal cholinergic axonal projections transport Aβ or APP to layer III of RSg.

Keywords

acetylcholinesterase; axonal transport; basal forebrain; lesions; synaptic drive

Address for correspondence: Richard T. Robertson, Department of Anatomy and Neurobiology, School of Medicine, University of California, Irvine, California 92697-1280 USA, telephone: 7949-824-6553 fax: 949-824-1105 rtrobert@uci.edu.
Section editor: Dr. Miles Herkenham

The presence in the brain of beta amyloid (Aβ) plaques is one of the hallmark characteristics of Alzheimer's disease (AD) (Glenner and Wong, 1984; Hardy and Higgins, 1992; Selkoe, 1996; Auld et al., 2002; Hardy, 2006). Amyloid plaques are made up primarily of the 42-amino acid sequence peptide known as Aβ, which accumulates both intracellularly and extracellularly, (Weidemann et al., 1989; LaFerla et al., 2007). Both intracellular Aβ and extracellular plaque accumulations of Aβ have been shown to be damaging to neurons (Walsh and Selkoe, 2004; Cleary et al., 2005; Lesne et al., 2006). While it is generally agreed that the A is released into extracellular space, it is not clear whether the Aβ is released preferentially from neuronal somata or dendrites, and it is not clear under what conditions the Aβ may be transported along axons and released from synaptic terminals.

Gaining an understanding of the cellular mechanisms underlying Alzheimer's disease is dependent upon an understanding of how APP and Aβ are produced and processed in the brain. One method of studying the neurobiology of Alzheimer's disease involves the generation of transgenic models (Wilcock and Colton, 2008); towards this end, a triple transgenic mouse strain (3xTg-AD) that harbors the mutant transgenes for alleles of presenilin 1, amyloid precursor protein (APP), and tau has recently been developed (Oddo et al., 2003). Mature 3xTg-AD mice display prominent levels of Aβ immunoreactivity as well as tau immunoreactivity in forebrain regions. Analyses of cerebral cortical tissue from 3xTg-AD mice of varied ages has demonstrated that Aβ is first seen intracellularly in neurons and later as extracellular plaque deposits (Oddo et al., 2003a;b). These 3xTg-AD mice display several critically important features of AD, including behavioral impairments that correlate with Aβ levels (Billings et al., 2005; Oddo et al., 2006).

Utilizing transgenic models such as the 3xTg-AD mouse strain offers a valuable opportunity to study in detail the neurobiology of Aβ accumulation. Perusal of a library of material revealed a curious interesting pattern of Aβ immunoreactivity in layer III of retrosplenial cortex of these 3xTg-AD mice. This Aβ immunoreactivity occurs as a band that appears similar to a laminar axonal terminal field in cortex. The goal of the present study was to study this pattern of Aβ, to determine its relationship to the axonal terminal field from the medial septum and diagonal band, and to determine whether disrupting this system of axonal afferents would interfere with Aβ production or immunoreactivity.

EXPERIMENTAL PROCEDURES

Animals

These experiments used adult mice of the triple transgenic strain (3xTg-AD) developed by Oddo and LaFerla (Oddo et al., 2003). In generating these transgenic mice, human amyloid precursor protein (APP) cDNA harboring the Swedish mutation (KM670/671NL) and human four-repeat *Tau* harboring the *P301L* mutation were co-microinjected into single-cell embryos of homozygous presenilin 1 ($PS1_{M146V}$) knockin mice. The background of the PS1 knockin mice was a hybrid 19/C57BL6 strain. The transgenic mice used in this study were all of the same genetic and strain background, and were drawn from the colony maintained by the LaFerla laboratory in the UC Irvine Gillespie Neuroscience Facility vivarium. Images were obtained from a library of slides of 15 of the 3xTg-AD mice, euthanized at ages 9 mo to 23 mo, from the LaFerla laboratory; in addition, 24 3xTg-AD animals aged 12 to 22 months were used in experiments involving survival surgery. Further, studies of normal connections of retrosplenial cortex and studies of basal forebrain lesions were undertaken in 32 control non-transgenic adult mice (termed wild type mice) of the C57BL6 strain, purchased from Charles River (Wilmington MA). Axonal tracing experiments using DiI used 17 C57BL6 mice 12–15 days of age, born in the laboratory from pregnant dams purchased from Charles River. All mice were housed in a satellite vivarium, kept on a 12 hr light: 12 hr dark schedule, and had *ad libitum* access to standard lab chow and water.

All procedures were carried out in accordance with the National Institutes of Health Guide for the Care and Use of Laboratory Animals, and were approved by the University of California, Irvine, Institutional Animal Care and Use Committee. All efforts were made to minimize animal suffering and to use only the number of animals necessary to produce reliable scientific data.

Materials

Reagents were purchased from Sigma Chemical Co. (St Louis, MO, USA) unless otherwise noted.

Surgical Procedures

Wild type (wt) and 3xTg-AD mice were deeply anesthetized with one of several different anesthetics, including sodium pentobarbital (40 mg/kg; IP), a mixture of Ketamine and Xylazine (40 mg/kg Ketamine and 4 mg/kg Xylazine; IP), or Avertin (250 mg/kg; IP) and placed in a stereotaxic apparatus. Electrolytic lesions were placed in the medial septum and nucleus of the diagonal band of 12 mice, aged 12–14 mo (8 mice) or 19–20 mo (4 mice) 3XTg-AD mice and 14 C57BL6 wt mice. Stereotaxic coordinates, (based on the atlas of Paxinos and Franklin, 2004) referenced from bregma were: AP: 0.8 mm; ML: 0.3 mm; DV: -4.0 and -5.0 mm.

Four wt and four 3xTg-AD mice were prepared for immunolesions of basal forebrain cholinergic neurons. Injections of 1 μl of a murine p75-SAP toxin (Advanced Targeting Systems, San Diego CA) at1.86 μg/μl of saline were made unilaterally into the lateral ventricle (stereotaxic coordinates AP: 0; ML: 0.8 mm; DV: − 2. mm). The toxin was infused over a period of 2 min, and the needle left in place for 3–5 min before withdrawing.

In 10 other wt mice and 7 other 3xTg-AD mice, the cingulate bundle was cut at the level of bregma, using a #11 scalpel blade inserted 1.4 mm below the pial surface, between 0.2 and 1 mm lateral to the midline.

For all surgical procedures, any bleeding was controlled with Gelfoam, the surgical wound sutured, and the animal maintained under a warming lamp until normal motility returned and then returned to the home cage.

At the time of euthanasia, animals were deeply anesthetized with sodium pentobarbital (100 mg/kg). A peristaltic perfusion pump, with a flow rate of 5 ml/minute, was used to perfuse the animals through the heart with 0.9% saline followed by 4% paraformaldehyde in 0.1M sodium phosphate buffer, pH 7.2. Brains were removed, postfixed overnight, and then transferred to 30%sucrose for cryoprotection.

Immunocytochemistry

Sections cut from basal forebrain and posterior cortex using a freezing sledge microtome (25–40 μm) or Vibratome (50 μm) were processed for ChAT or p75 receptor immunocytochemistry. Sections were blocked with 3% normal serum (rabbit serum for ChAT; goat serum for p75) for 1 hr at room temperature. Sections were then incubated overnight at 4°C in either goat anti-ChAT (Chemicon AB144P; Milipore-Chemicon, Temecula CA) primary antibody, 1:500 in normal rabbit serum or in rabbit anti-p75 receptor primary antibody (a generous gift from Dr. L. Reichardt); 1:50,000 in normal goat serum. Triton X-100 (at 0 .25%) was included in both incubation media. Sections were rinsed in sodium-phosphate buffered saline (PBS) and then incubated in biotinylated secondary antibody (1:200) for 1 hr at room temperature; Secondary antibodies (from Vector Labs, Burlingame CA) were rabbit anti-goat for the ChAT procedure or goat anti-rabbit for the p75. Sections were stained according to the Vectastain Elite ABC

Kit from Vector laboratories, using nickel-intensified DAB as the chromagen. Sections were mounted, dehydrated, cleared in xylenes, and coverslipped for examination under the light microscope.

Immunocytochemical procedures to reveal Aβ were carried out on 40–50 μm thick transverse sections of 3xTg-AD mouse brains, cut on either a freezing microtome or on a Vibratome. For most experiments, free floating sections were treated with 88% formic acid for 7 min, rinsed 3X in PBS, and then blocked in normal goat serum for 1 hr and incubated overnight in antibody (β-amyloid 1–16 monoclonal antibody; Signet SIG-39322 from Covance, Emeryville CA; diluted 1:1000 in PBS with goat serum). Other studies used the OC β-amyloid antibody from C. Glabe (Kayed et al., 2007; a rabbit polyclonal antibody, diluted at 1:5000); the procedure for this antibody was similar to the procedure for the SIG-39322 antibody, but omitted the formic acid treatment. After incubation, sections were rinsed in PBS and then placed for 1 hr in a biotinylated goat anti-mouse secondary antibody or a biotinylated goat anti-rabbit secondary antibody (both from Vector Labs), diluted 1:200 in goat serum. Sections then were rinsed 3X in PBS, processed using the ABC kit (Vector Labs) and reacted in 0.2% diamino benzidine and 0.003% H_2O_2. Sections were rinsed again and mounted on gelatin coated slides and cover slipped with DPX mounting medium. Control sections, processed with either the primary or secondary antibody omitted, revealed no labeling.

AChE Histochemistry

Brains were cut in the transverse plane at thickness of 40–50 μm and processed for AChE histochemistry as described by Hedreen et al. (1985). Slices were rinsed in 100 mM acetate buffer, (pH 6.0) (3X, 10min) and then incubated in 50 ml of a solution made with 25mg acetylthiocholine iodide, 1ml 5 mM tetraisopropyl pyrophosphoramide, 5 ml of 30 mM copper sulfate, and 1 ml 5 mM potassium ferricyanide in acetate buffer (pH 6.0). After 2 hr of incubation in darkness, the tissue was rinsed in five changes of 100 mM acetate buffer and then reacted in 1% ammonium sulfate. Following 5 rinses in 0.1M sodium nitrate, sections were reacted in 0.1% silver nitrate for 5 minutes or until fibers were clearly visible in cortex. Sections were then rinsed in sodium nitrate followed by rinses in acetate buffer and mounted on slides. Selected sections were counterstained with cresyl violet to document the relationship between AChE positive axons and local cytoarchitecture.

DiI Preparations

Studies of axonal connections were performed on twenty C57BL6 wt mice and two 3xTg-AD mice, aged 12–15 days. These animals were deeply anesthetized with sodium pentobarbital and perfused transcardially with 4% paraformaldehyde in 0.1 M sodium-phosphate buffer. The brains were postfixed for at least 2 days in 4% paraformaldehyde. Brains received placements of 1,1′,dioctadecyl-3,3,3′,3-tetramethylindocarbocyanine perchlorate (DiI; Molecular Probes Invitrogen, Carslsbad CA).

After fixation, 6 of the w.t. brains and one 3xTg-AD brain were divided into two hemispheres by a mid-sagittal cut. Each hemisphere received placement into the septum, using a medial approach, of a very small crystal of DiI (Molecular Probes, Eugene, OR). The other brains received unilateral or bilateral placements of DiI directly into retrosplenial cortex. To label the retrosplenial cortex, placements were made into the medial wall of the cortex, close to the level of the splenium of the corpus callosum. Use of fine glass pipettes under a dissection microscope aided the placement of small DiI crystals. Tissue with DiI placements was stored in PBS and 0.2% azide solution at 37°C for 4–6 weeks. Tissue blocks then were embedded in 3% agarose solution and Vibratome sections were cut in the transverse plane at a thickness of 100 μm. Some sections were counter-stained with ethidium bromide or BoPro (Molecular Probes; Eugene OR).

Wet mounted sections were viewed with a Nikon epifluoresence microscope equipped with rhodamine, fluorescein, and ultraviolet filter sets. Retrogradely labeled cells and anterogradely labeled axons were compared to local cytoarchitecture, as visualized from ethidium bromide or BoPro stains of the same sections.

Photographic and Illustration Techniques

Immunocytochemically or histochemically stained sections were examined under bright field or fluorescence microscopy. Photographic images were taken using a Nikon Optiphot with a Nikon DS 5M digital camera and imported into Photoshop. Contrast and brightness were adjusted for photographs within the same plate; no other manipulation of the images was done.

RESULTS

Presence of Aβ immunoreactivity in granular retrosplenial cortex

The granular retrosplenial cortex (RSg) is located along the medial wall of the posterior cingulate gyrus (Krieg, 1943). The cytoarchitecture of RSg features a distinctive dense granular layer II (Krieg, 1943; Vogt and Peters, 1981), as illustrated by the photomicrograph of a Nissl stained section in Figure 1A. Approximately half of the RSg is situated, as its name implies, caudal to the splenium of the corpus callosum, but RSg also extends anteriorly to the splenium, along the ventral cingulate gyrus. Histochemically reacted sections demonstrate that the RSg also displays a characteristic dense pattern of AChE activity in layer III, as illustrated in Figure 1B. This band of AChE activity is seen throughout the anterior-posterior and medial-lateral extents of RSg. The dense granular layer II seen in Nissl stained sections and the dense pattern of AChE in layer III both are characteristic of normal wild type mice and also of the 3xTg-AD mice. The band of AChE seen in cortical layer III corresponds to a band that also labels for choline acetyltransferase (ChAT) immunocytochemistry, as illustrated in figures 1C and 1D. Sections from 3xTg-AD mice that are older than approximately 18 months of age, and processed for Aβ immunoreactivity, demonstrate Aβ positive cells, primarily in deeper cortical layers, and also a prominent band of Aβ immunoreactivity in layer III of RSg (fig. 1E).

The band of Aβ immunoreactivity in layer III appears quite different from the Aβ immunoreactivity that can be seen within cells in the deeper layers of RSg and in cells and extracellular plaques elsewhere in the cerebral cortex. The Aβ immunoreactivity in layer III of RSg of older animals occurs as a distinct lamina, and appears similar to the pattern of an axonal terminal field. The band of Aβ immunoreactivity in cortical layer III, like the pattern of AChE histochemical reaction product in layer III, is characteristic of RSg, throughout its anterior-posterior and medial-lateral extents, as illustrated by the photomicrographs of sections taken from a 20 mo animal, as shown in figure 2A–C.

Although the 3xTg-AD mice display Aβ immunoreactivity within cortical pyramidal cells by about 4 months of age, and extracellular plaques are seen in some regions of cerebral cortex by about 6 months of age (Oddo et al., 2003), the band of Aβ immunoreactivity in RSg appears relatively late in the 3xTg-AD animal's life. As shown in Figure 2D, the Aβ band is not detectable by these immunocytochemical techniques in animals euthanized at 13 months of age; at this age, however, Aβ positive neurons are scattered in the deeper layers of RSg cortex and extracellular plaques are clearly visible in the subiculum. By 18 months of age (Fig. 2E) the band of Aβ immunoreactivity can be seen in layer III, and by 20 months (Fig. 2E) the band is quite distinct. At no age were Aβ positive cells prominent in the superficial layers (layers I-IV) of RSg cortex, although Aβ positive pyramidal cells were detected consistently in deeper cortical layers in animals older than 12 months.

Basal forebrain projections to retrosplenial cortex

The pattern of Aβ immunoreactivity in layer III is suggestive of an axonal terminal plexus. Further, the similarity of the pattern of Aβ immunoreactivity and the patterns of AChE histochemical reaction product and ChAT immunoreactivity suggests that the putative terminal plexus may be that of axons from basal forebrain cholinergic neurons (Bigl et al., 1982; Lysakowski et al.,1989). The next set of experiments explored the identity of candidate axonal projections. Retrograde axonal labeling using the lipophilic tracer DiI was used in experiments to reveal basal forebrain projections to RSg cortex. Figure 3A shows the area of cortex directly labeled by a placement of a small DiI crystal in retrosplenial cortex of a P15 wt mouse; retrograde labeling of axons and cells by DiI is illustrated in Figures 3B,C,C_1,C_2. Retrogradely labeled cells were detected in medial septum and the vertical limb of the nucleus of the diagonal band, confirming studies in other species (Wenk et al., 1980; Bigl et al., 1982; Tengleson et al., 1992). The location of these retrogradely labeled neurons was used to identify sites for placement of DiI crystals for anterograde demonstration of basal forebrain projections to cortex. Placements of small crystals of DiI were made in medial septum (as illustrated in Figure 3D) or in nDB. Labeling of axon terminal fields was detected in RSg cortex as a distinct band of DiI in layer III, as illustrated in Figure 3E. Note that the areal and laminar patterns of axonal labeling in RSg from a septal placement of DiI appear remarkably similar to the pattern of endogenous AChE or ChAT and also to the pattern of Aβ immunoreactivity.

Effects of basal forebrain lesions on Aβ immunoreactivity in RSg

If the pattern of Aβ immunoreactivity in RSg is associated with the terminal field of axons from cholinergic neurons in the basal forebrain, then eliminating those cholinergic axons would be expected to affect the pattern of Aβ expression. The next set of experiments investigated this possibility. Electrolytic lesions were placed in medial septum and/or the nDB of 19 C57BL6 wt mice and of 8 of the 3xTg-AD mice aged 10–18 mo. Figure 4 presents results from a case in which the lesion (Fig. 4A) was placed in a 3xTg-AD mouse at 12 months of age (before the pattern of Aβ immunoreactivity appears in RSg). This animal was euthanized and studied at 20 months of age. Figure 4B demonstrates that this lesion of septum and diagonal band was followed by a loss of AChE histochemical reaction product in layer III of the ipsilateral RSg, confirming earlier reports in other species (Tengelson et al, 1992). More importantly, Figure 4C demonstrates that Aβ immunoreactivity, normally characteristic of RSg, is absent in the left hemisphere sustaining the lesion, although normal patterns are present in the right, control hemisphere. Figure 4D presents results from another case with an incomplete septal lesion, with markedly reduced Aβ immunoreactivity in the operated (left) hemisphere. Interestingly, although the band of Aβ immunoreactivity was lost, or markedly reduced, following placement of lesions in the medial septum and diagonal band, Aβ immunoreactivity in neurons of RSg was not affected.

Animals (N=2) that received a surgical knife cut lesion of the cingulate bundle at ages younger than 12 mo also displayed a unilateral absence of the Aβ immunoreactivity in RSg cortex (results not illustrated).

Effects of short term septal or cingulate bundle lesions on Aβ immunoreactivity in RSg of older mice

Electrolytic lesions were placed in the medial septum and nucleus of the diagonal band (N=4), or surgical knife cuts were made in the cingulate bundle (N=5) of 3xTg-AD mice at ages at which the patterns of Aβ immunonreactivity would already have appeared in RSg cortex (at 19–20 mo). Animals were euthanized and tissue collected at post-lesion survival periods of 2–4 weeks. Lesions, such as the knife cut illustrated in figure 5A, placed in these older animals resulted in marked and rapid reduction of AChE histochemical activity in layer III of RSg, as illustrated in figure 5B. Cytoarchitecture as revealed by Nissl stains (fig. 5C) showed normal

cortical layers, so loss of AChE is not due to degenerated tissue. These lesions did not eliminate the pattern of Aβ immunoreactivity in layer III of RSg, although cases with longer survival periods (4 weeks compared to 2 weeks) showed reduction in Aβ immunoreactivity (Fig. 5D).

Effects of immunolesioning of basal forebrain cholinergic neurons

Electrolytic lesions and surgical transactions of axonal pathways are non-specific, in that they impact the population of cells or axons, irrespective of neurochemical phenotype. To test whether the AChE axonal plexus in layer III of RSg is indeed cholinergic, and to test whether it is the loss of cholinergic afferents that impacts the axonal plexus and the Aβ immunoreactivity in RSg, the basal forebrain cholinergic system was damaged using the immunolesioning method (Robertson et al., 1998; Berger-Sweeney et al., 2001). Results from an animal that received a unilateral injection of the p75 SAP toxin at 18 mo and then euthanized 4 weeks later at 19 mo are illustrated in figure 6.

Figure 6A and B illustrate the marked unilateral loss of cholinergic (in this example, p75 positive) neurons in the medial septum following the unilateral injection. Note that a few neurons remain in the right hemisphere. Figure 6C illustrates a marked loss of AChE positive axons in the corresponding (right) RSg, while fig. 6D reveals a corresponding marked loss of p75 immunoreactivity. Although the p75 labeling lacks the clear axonal appearance of the AChE histochemical reaction, the overall patterns are similar. Similar to the results shown in fig. 5, fig. 6E demonstrates a reduction of Aβ immunoreactivity in this animal.

Relationship between AChE positive neurons and Aβ immunoreactivity in Septum

The evidence presented above indicates that a medial septal lesion placed before the appearance of the band of Aβ immunoreactivity in layer III of RSg results in the absence of the Aβ in the corresponding hemisphere. This finding suggests that Aβ may be produced by septal neurons and transported along their axons to the terminal fields in RSg. Supportive evidence for this notion would be offered by co-localization of Aβ immunoreactivity and cholinergic markers in the medial septum. This possibility was investigated, and Figure 7 presents results taken from the septum of a 3xTg-AD mouse, euthanized at 23 mo.

Figures 7A and 7D show a section taken through the septum and processed for ChAT immunocytochemistry. Note the strongly immunoreactive neurons in the medial septum (MS) but absence of ChAT positive neurons more laterally. Figures 7B and 7D show an adjacent section, processed histochemically for AChE. Although the AChE histochemical reaction product is more diffuse and does not have the clear cellular appearance of the ChAT immuoreactivity, the distributions within the septal complex of the two are similar. In contrast, figures 7C and 7F illustrate that dense Aβ positive plaques are characteristic of the lateral septal region, while the medial septum shows no immunoreactivity. Clearly, Aβ immunoreactivity is found in different regions of the septal complex than those occupied by cholinergic neurons.

DISCUSSION

Choice of neural model system

Investigators have studied axonal transport of APP in several model systems, including the peripheral nervous system (Koo et al., 1990; Sisodia et al, 1993), optic nerve (Amaratunga and Fine, 1995), cultured hippocampal neurons (Ferreira et al., 1993; Kaether et al., 2000) and in the perforant pathway from the entorhinal cortex to the dentate gyrus (Buxbaum et al., 1998; Lazarov et al., 2002). The neural system examined in the current study offers the advantage of a clearly defined laminar pattern of Aβ in a defined region of cerebral cortex, and the added advantage that the Aβ pattern corresponds to a demonstrated axonal terminal field. It is of further interest that many, and perhaps all, of the cells of origin of this axonal terminal field

are cholinergic, a potentially important point in light of observations that cholinergic neurons appear to be among those most affected in Alzheimer's disease (Davies and Maloney, 1976; Bartus et al., 1982; Coyle et al., 1983; Kasa et al., 1997; Hu et al., 2003; Lüth et al., 2003; Lyness et al., 2003; Rees et al., 2003; Mesulam 2004; Pakaski and Kalman, 2008).

The cholinergic projections of interest here form a part of the broad system of basal forebrain projections to cerebral cortex. In human brain, the cholinergic neurons cluster together to form the nucleus basalis, but in rodent brain the cholinergic neurons are found scattered through several nuclear groups of the basal forebrain, including the medial septum, the nucleus of the diagonal band, the ventral medial globus pallidus, and portions of the hypothalamus (Lewis and Shute, 1967; Wenk et al., 1980; Bigl et al., 1982; Mesulam et al., 1983; Butcher and Woolf, 2004). These cholinergic neurons send rather broad axonal projections to cortical structures, but the projections do display an underlying loose topographic organization. Projections to the RSg originate in the medial septum and the vertical limb of the nucleus of the diagonal band as has been demonstrated in several species (Bigl et al., 1982; Mesulam, 1983; Butcher and Woolf, 2004) including mouse (present study). Although AChE is not always a valid indicator of cholinergic neurons (Lehman and Fibiger, 1979; Robertson and Yu, 1993) virtually all basal forebrain cholinergic neurons (defined as expressing choline acetyltransferase) do express AChE (Levey et al., 1983). Further, laminar patterns of AChE histochemical activity in RSg correspond to laminar patterns of other cholinergic markers, including ChAT immunoreactivity and p75 receptor immunoreactivity. Finally, immunolesioning of basal forebrain cholinergic neurons strongly reduces AChE positive axons as well as the specific cholinergic markers ChAT and p75 immunoreactivity. Thus, we believe AChE histochemistry is both a reliable and a valid marker for basal forebrain derived cholinergic projections to RSg.

Cellular localization of Aβ

The origin and distribution of much of the Aβ detected in the cerebral cortex of 3xTg-AD mice has been described by Oddo, LaFerla and colleagues, with Aβ immunoreactivity first detected intracellularly in cortical pyramidal neurons, and later is found associated with extracellular plaques (Oddo et al., 2003a;b). The Aβ peptides are derived from the amyloid precursor protein (APP) through endoproteolytic cleavage actions, the last of which is performed by gamma secretase to produce the Aβ (Weidemann et al., 1989). Gamma secretase, and hence ultimately Aβ production, may be active intracellularly or at the neuronal membrane. The antibodies used in the present study produced similar patterns of immunoreactivity. The Signet 39322 antibody is believed to react with all isoforms of Aβ, and the OC antibody reacts with fibrillar amyloid Aβ, but not the APP (Kayed et al., 2007).

It is believed that the Aβ is released from intracellular compartments to form the extracellular deposits recognized as the amyloid plaques. The band of Aβ immunoreactivity in layer III of RSg, however, does not display a clear spatial or temporal relationship with Aβ positive neurons within RSg. Indeed, although Aβ positive neurons are seen prominently in deep layers of RSg, Aβ positive neurons are rare in the superficial layers (see Figs. 1,2). It is conceivable that apical dendrites of Aβ positive pyramidal neurons in deep layers of cortex could release the Aβ into cortical layer III, but dendritic transport and release has not been reported and seems to us to be unlikely. Further, placement of lesions in medial septum or immunotoxin damage to septal cholinergic neurons reduce Aβ immunoreactivity in layer III, but have no observable affect on Aβ in deeper neurons.

The remarkable similarity of the pattern of Aβ immunoreactivity and the pattern of basal forebrain derived cholinergic axon terminals is strongly suggestive of a relationship between cholinergic axons and the band of Aβ. The precise nature of this putative relationship remains unclear, but possibilities include: 1) activity in the cholinergic terminals is able to induce Aβ expression and subsequent release by cortical cells; and 2) the Aβ or APP is transported to RSg

along cholinergic axons, and the Aβ is found within or released by those cholinergic axon terminals.

In the case of the first possibility, the cholinergic axons from the basal forebrain could stimulate local RSg cortical neurons to produce APP that would then be cleaved to form the Aβ. Studies have demonstrated that neural activity is capable of driving expression of a variety of receptor and other proteins (Tang and Schuman, 2002; Bramham and Wells, 2007), and investigators have demonstrated that neural activity can modulate formation and secretion of Aβ peptides in a dissociated cell culture system (Kamenetz et al., 2003). In this scenario, the results from experimental damage to the basal forebrain would be interpreted as demonstrating that the loss of the afferent input results in reduced synaptic drive and consequently reduced APP and Aβ production. This possibility seems to us to be unlikely because, as noted above, very few Aβ positive neurons are present in the superficial layers of RSg and release of Aβ from dendrites of deeper pyramidal neurons has not been described. Further, as noted above, damage to cholinergic neurons in basal forebrain affect Aβ immunoreactivity in layer III, but does not affect Aβ immunoreactivity in deeper cortical neurons. In aggregate, these results suggest that the Aβ does not accumulate in layer III as a result of release from deeper neurons. Further studies will be necessary to determine the locus of production of the Aβ in this neural circuit.

The second possibility is that the Aβ may be located within, and possibly released by, cholinergic axons from basal forebrain neurons. Other investigators have demonstrated that the APP can be actively transported by axonal transport mechanisms (Koo et al., 1990; Ferreira et al., 1993; Buxbaum et al., 1998; Lazarov et al., 2002). The present experimental results are compatible with this idea. Damage to cholinergic neurons in basal forebrain, at a time before the Aβ immunoreactivity normally appears in RSg, results in absence of the pattern of Aβ in layer III and also absence of the corresponding band of cholinergic markers. The loss of Aβ immunoreactivity from cortical layer III is not accompanied by change in the number or apparent staining intensity of Aβ in cortical neurons. Several methods of producing damage to the basal forebrain projections, including placement of electrolytic lesions in the basal forebrain, immunotoxin mediated lesions of basal forebrain cholinergic neurons, and lesions in the cingulate bundle (through which the cortically projecting basal fore brain derived axons pass; Wenk 1980; Bigl et al., 1982; Tengelsen et al., 1992) at ages after the appearance of the band of Aβ do not result in the immediate loss of the band of Aβ immunoreactivity, although the corresponding band of cholinergic axon markers is lost. This result suggests that while the AChE is found as part of the cholinergic axon terminals from basal forebrain, the Aβ is likely to be outside of the axon terminals *per se*. If the Aβ is continually, albeit slowly, deposited in layer III of RSg from cholinergic terminals and the deposited Aβ is continually, and again slowly, removed by phagocytic cells in the region, then it would be expected that damage to cholinergic axons later in the animal's life (after 18 mo) would eventually lead absence of Aβ in RSg.

In aggregate, these results and this line of reasoning would posit that the Aβ, or its precursor APP, is produced in cell bodies in the basal forebrain and transported along axons to the terminals in RSg. If this pathway is removed by damage early in the animal's life, the pattern of Aβ immunoreactivity never appears. Later in life, after the Aβ pattern can be detected in the extracellular milieu, lesions interrupting the afferents do not lead to short term elimination of the Aβ that already has been deposited. However, if extracellular Aβ levels normally result from some balance of ongoing deposition and ongoing removal by phagocytic cells (Schenk et al., 1999; Yazawa et al., 2001), damage to cholinergic afferents in older animals likely would lead to eventual clearing by local cells. Indeed, figure 6 demonstrates that in an animal receiving cholinergic insult at 18 months, levels of Aβ in RSg are notably lowered one month later.

Information missing from this scenario, however, is evidence that APP or Aβ is produced by cortically projecting neurons of the medial septum. It is of interest that strong immunoreactivity for Aβ is seen in the lateral septum, but not in the medial septum. It is the medial septum that contains cholinergic neurons (Wenk et al., 1980; Bigl, et al., 1982; Mesulam et al., 1983; figure 7 here), the axons of which project to layer III of RSg. The lack of correspondence between the location of Aβ immunoreactivity in the septum and the locus of origin of the axonal projection to RSg may decrease enthusiasm for the Aβ transport hypothesis. However, absence of Aβ immunoreactivity in the medial septum does not necessarily mean that the APP is not produced by these cells, because neither of the Aβ antibodies used in the present studies appears to recognize APP. Further, although we investigated antibodies to APP, we were not able to convince ourselves that the APP immunoreactivity demonstrated only the transgenic human APP in preference to normal endogenous mouse APP (data not shown). As in other systems (Koo et al., 1990; Ferreira et al., 1993; Buxbaum, 1998; Lazarov et al., 2002) APP could be produced by medial septal cells and transported along their axons, to be cleaved to immunocytochemically detectable Aβ in the region of the axon terminals.

The present results are somewhat analogous to those reported previously by the Sisodia laboratory (Buxbaum et al., 1998; Lazarov et al., 2002). These investigators studied possible transport of Aβ, or its precursor protein, from the entorhinal cortex to the dentate gyrus in a different transgenic mouse model that also expresses patterns of Aβ immunoreactivity. These investigators report that damage to the perforant path axons results in a reduction in Aβ immunoreactivity in the ipsilateral dentate gyrus, as well as other regions of the ipsilateral hippocampal formation. The authors attribute this reduction to the reduction of deposition of Aβ (or its precursor) in the dentate gyrus, while the removal by local macrophages of existing deposits of Aβ continues unabated. Interestingly, the authors report that severing the axons of the perforant path in young animals, before the time the Aβ deposits appear in the dentate gyrus, does not interfere with the appearance of Aβ immunoreactivity four months later. The authors suggest that the truncated axons are able to sprout new branches that will reinervate the dentate and transport the Aβ to the reinnervated terminal zone site. In the present studies, the neurons of origin of the projection were eliminated by electrolytic or immunotoxin lesions, and hence could not recover to regenerate new cortically projecting axons.

Relationship of Aβ and neural degeneration

Several recent studies (Jaffar et al., 2001; German et al., 2003; Hu et al., 2003; Aucoin et al., 2005) have reported cholinergic deficits associated with presence of Aβ in other mouse transgenic models of Alzheimer's disease. These studies indicate that the presence of fibrillary Aβ in plaques exerts a deleterious affect on cholinergic and other axons, and that diffuse Aβ, perhaps that is not recognizable by currently used antibodie, may have a more specific damaging affect on cholinergic axons. These results raise the interesting question of whether the presence of Aβ in layer III of RSg causes damage to the cholinergic axons in that region, or whether those cholinergic axons play a role in the production of the Aβ.

Role of Aβ in Alzheimer's disease

An understanding of how Aβ is released and subsequently processed extracellularly will be important for understanding the damaging effects that Aβ has on neuronal tissue, and hence potentially for the pathogenesis of Alzheimer's disease (Cleary et al., 2005). In this regard, the fine structural localization of the Aβ immunoreactivity would be of great interest, particularly in regard to whether it is found within or around axon terminals (Yamaguchi et al., 1989; Ikin et al., 1996) from the septum, or within cortical neurons in layer III of RSg cortex. An association between Aβ and cholinergic terminals would be particularly intriguing in light of the finding that amyloid plaques often display AChE or nonspecific cholinesterase activity (Wright et al., 1993; Guillozet et al., 1997). The Aβ that is deposited likely eventually will be

transformed to a plaque that is associated with degeneration of neurites, including the degeneration of cholinergic circuitry (Wright et al., 1993; Kasa et al., 1997; Auld et al, 2002; Hu et al., 2003; Lüth et al., 2003).

While disruptions in amyloid production constitute important genetic factors in the pathogenesis of AD (Selkoe, 1991; Hardy and Selkoe, 2002; Lesne et al., 2006), it is also clear that the deposited amyloid plaques alone do not account for the neuronal degeneration and cognitive losses that characterize AD (Masters et al., 1985; Arrigada et al., 1992; Naslund et al., 2000; McLean et al., 2001; Billings et al., 2005; Oddo et al., 2006). Loss of synaptic structure and function form the neuropathological bases of dementia (Terry et al., 1991; Honer et al., 1992; Dickson et al., 1995; Sze et al., 1997; Selkoe, 2002;), but the cause of the loss of synapses in AD remains somewhat unclear. Although much attention has been directed towards the amyloid plaques, soluble levels of Aβ and vascular Aβ also have been demonstrated to be important (Masters et tal., 1985; Naslund et al., 2000; McLean et al., 2001; Thal et al., 2008) and indeed soluble levels of Aβ more closely correlate with human cognitive decline than does amyloid plaque load (Terry et al., 1991; Wang et al., 1999). Although the presence of amyloid plaques does not correlate well with scales of dementia (Wang et al., 1999; Naslund et al., 2000; McLean et al., 2001), some combination of deposited and soluble amyloid appear to be the main causative agents in cognitive decline. Hence, the amyloid cascade hypothesis (Hardy and Higgins, 1992; Hardy, 2006; LaFerla et al., 2007), featuring a central pathological role of amyloid, remains a leading theory of Alzheimer pathology.

Acknowledgments

Supported in part by Alzheimer's Association grant IRG 06-25497 to RTR, NIH grant NS 30109 to RTR, and NIH grant AG-02754 to FML. We thank Drs. Salvatore Oddo, Kim Green and Mathew Blurton-Jones for providing 3xTg-AD mice and for thoughtful discussions. We also thank Dr. Charles Glabe for the gift of the OC antibody and Dr. Louis Reichardt for the gift of the p75 antibody.

List of Abbreviations

Aβ	amyloid beta peptide
AC	anterior commissure
AD	Alzheimer's disease
AchE	acetylcholinesterase
APP	amyloid precursor protein
ChAT	choline acetyltransferase
CC	corpus callosum
DiI	1,1′,dioctadecyl-3,3,3′,3-tetramethylindocarbocyanine perchlorate
Lat S	lateral septum
Med S	medial septum
nDB	nucleus of diagonal band
P	postnatal day
p75	low affinity nerve growth factor receptor
PBS	sodium-phosphate buffered saline

RSg	retrosplenial cortex, granular division
S	septum
Str	striatum
wt	wild type

References

Amaratunga A, Fine RE. Generation of amyloidogenic C-terminal fragments during rapid axonal transport in vivo of beta-amyloid precursor protein in the optic nerve. J Biol Chem 1995;270:17268–17272. [PubMed: 7542234]

Arriagada PV, Growdon JH, Hedley-Whyte ET, Hyman BT. Neurofibrillary tangles but not senile plaques parallel duration and severity of Alzheimer's disease. Neurology 1992;42:631–639. [PubMed: 1549228]

Aucoin J-S, Jiang P, Aznavour N, Tong X-K, Buttini M, Descarries L, Hamel E. Selective cholinergic denervation, independent from oxidative stress, in a mouse model of Alzheimer's disease. Neuroscience 2005;132:73–86. [PubMed: 15780468]

Auld DS, Kornecook TJ, Bastianeto S, Quirion R. Alzheimer's disease and the basal forebrain cholinergic system: relations to b-amyloid peptides, cognition, and treatment strategies. Progr Neurobiol 2002;68:209–245.

Baratta J, Ha DH, Yu J, Robertson RT. Evidence for target preferences by cholinergic axons originating from different subdivisions of the basal forebrain. Dev Brain Res 2001;132:15–21. [PubMed: 11744103]

Bartus RT, Dean RL III, Beer B, Lippa AS. The cholinergic hypothesis of geriatric memory dysfunction. Science 1982;217:408–414. [PubMed: 7046051]

Berger-Sweeney J, Stearns NA, Murg SL, Floerke-Nashner LR, Lappi DA, Baxter MG. Selective immunolesions of cholinergic neurons in mice: effets on neuroanatomy, neurochemistry, and behavior. J Neurosci 2001;21:8164–8173. [PubMed: 11588189]

Bigl V, Woolf NJ, Butcher LL. Cholinergic projections from the basal forebrain to frontal, parietal, temporal, occipital and cingulate cortices: a combined fluorescent tracer and acetylcholinesterase analysis. Brain Res Bull 1982;8:727–749. [PubMed: 6182962]

Billings LM, Oddo S, Green KN, McGaugh JL, LaFerla FM. Intraneuronal Ab causes the onset of early Alzheimer's disease related cognitive deficits in transgenic mice. Neuron 2005;45:675–688. [PubMed: 15748844]

Bramham CR, Wells DG. Dendritic mRNA: transport, translation and function. Nat Rev Neurosci 2007;8:776–789. [PubMed: 17848965]

Butcher, LL.; Woolf, NJ. Cholinergic neurons and networks revisited. In: Paxinos, G., editor. The Rat Nervous System. Vol. 3. Elsevier Academic Press; 2004. p. 1257-1268.

Buxbaum JD, Thinakaran G, Koliatsos V, O'Callahan J, Slunt HH, Price DL, Sisodia SS. Alzheimer amyloid protein precursor in the rat hippocampus: transport and processing through the perforant path. J Neurosci 1998;18:9629–9637. [PubMed: 9822724]

Cleary JP, Walsh DM, Hofmeister JJ, Shankar GM, Kuskowski MA, Selkoe DJ, Ashe KH. Natural oligomers of the amyloid-beta protein specifically disrupt cognitive function. Nat Neurosci 2005;8:79–84. [PubMed: 15608634]

Coyle JT, Price DL, DeLong MR. Alzheimer's disease: a disorder of cortical cholinergic innervation. Science 1983;219:1184–1190. [PubMed: 6338589]

Davies P, Maloney AJF. Selective loss of central cholinergic neurons in Alzheimer's disease. Lancet 1976;2:1943.

Dickson DW, Crystal HA, Bevona C, Honer W, Vincent I, Davies PP. Correlations of synaptic and pathological markers with cognition of the elderly. Neurobiol Aging 1995;16:285–298. [PubMed: 7566338]

Ferreira A, Caceres A, Kosik KS. Intraneuronal compartments of the amyloid precursor protein. J Neurosci 1993;13:3112–3123. [PubMed: 8331388]

German DC, Yazdani U, Speciale SG, Pasbakhsh P, Games D, Liang C-L. Cholinergic neuropathology in a mouse model of Alzheimer's disease. J Comp Neurol 2003;462:371–381. [PubMed: 12811807]

Glenner GG, Wong CW. Alzheimer's disease: initial report of the purification and characterization of a novel cerebrovascular amyloid protein. Biochem Biophys Res Commun 1984;120:885–890. [PubMed: 6375662]

Guillozet AL, Smiley JF, Mash DC, Mesulam M-M. Butyrylcholinesterase in the life cycle of amyloid plaques. Ann Neurol 1997;42:909–918. [PubMed: 9403484]

Hardy J. Alzheimer's disease: the amyloid cascade hypothesis: an update and reappraisal. Curr Alzheimer Res 2006;3:71–73. [PubMed: 16472206]

Hardy JA, Higgins GA. Alzheimer's disease: the amyloid cascade hypothesis. Science 1992;256:184–185. [PubMed: 1566067]

Hardy J, Selkoe DJ. The amyloid hypothesis of Alzheimer's disease: progress and problems on the road to therapeutics. Science 2002;297:353–356. [PubMed: 12130773]

Hedreen JC, Bacon SJ, Price DL. A modified histochemical technique to visualize acetylcholinesterase-containing axons. J Histochem Cytochem 1985;33:134–140. [PubMed: 2578498]

Honer WG, Dickson DW, Gleeson J, Davies P. Regional synaptic pathology in Alzheimer's disease. Neuribol Aging 1992;13:375–382.

Hu L, Wong TP, Cote SL, Bell KFS, Cuello AC. The impact of A -plaques on cortical cholinergic and non-cholinergic presynaptic boutons in Alzheimer's disease-like transgenic mice. Neuroscience 2003;121:421–432. [PubMed: 14522000]

Ikin AF, Annaert WG, Takei K, De Camilli P, Jahn R, Greengard P, Buxbaum JD. Alzheimer amyloid protein precursor is localized in nerve terminal preparations to Rab5-containing vesicular organelles distinct from those implicated in the synaptic vesicle pathway. J Biol Chem 1996;271:31783–31786. [PubMed: 8943215]

Jaffar S, Counts SE, Ma SY, Dadko E, Gordon MN, Morgan D, Mufson EJ. Neuropathology of mice carrying mutant APP_{swe} and/or$PS1M_{146L}$ transgenes: alterations in the $p75^{NTR}$ cholinergic basal forebrain septohippocampal pathway. Exper Neurol 2001;170:227–243. [PubMed: 11476589]

Kaether C, Skehel P, Dotti CG. Axonal membrane proteins are transported in distinct carriers: a two color video microscopy study in cultured hippocampal neurons. Mol Biol Cell 2000;11:1213–1224. [PubMed: 10749925]

Kamenetz F, Tomita T, Hsieh H, Seabrook G, Borchelt D, Iwatsubo T, Sisodia S, Malinow R. APP processing and synaptic function. Neuron 2003;37:925–937. [PubMed: 12670422]

Kasa P, Rakonczay Z, Gulya K. The cholinergic system in Alzheimer's disease. Progr Neurobiol 1997;52:511–535.

Kayed R, Head E, Sarsoza F, Saing T, Cotman CW, Necula M, Margol L, Wu J, Breydo L, Thompson JL, Rasool S, Gurlo T, Butler P, Glabe CG. Fibril specific, conformation dependent antibodies recognize a generic epitope common to amyloid fibrils and fibrillar oligomers that is absent in prefibrillar oligomers. Molec Neurodegen 2007;2:1–11.

Koo EH, Sisodia SS, Archer DR, Martin LJ, Weidemann A, Beyreuther K, Fischer P, Masters CL, Price DL. Precursor of amyloid protein in Alzheimer disease undergoes fast anterograde axonal transport. Proc Nat'l Acad Sci USA 1990;87:1561–1565.

Krieg WJS. Connections of the cerebral cortex. I. The albino rat. B. Structure of the cortical areas. J Comp Neurol 1943;84:277–323.

LaFerla FM, Green KN, Oddo S. Intracellular amyloid-β in Alzheimer's disease. Nature Rev Neurosci 2007;8:499–509. [PubMed: 17551515]

LaFerla FM, Oddo S. Alzheimer's disease: Abeta, tau and synaptic dysfunction. Trends Mol Med 2005;11:170–176. [PubMed: 15823755]

Lazarov O, Lee M, Peterson DA, Sisodia SS. Evidence that synaptically released b-amyloid accumulates as extracellular deposits in the hippocampus of transgenic mice. J Neurosci 2002;22:9785–9793. [PubMed: 12427834]

Lehmann J, Fibiger HC. Acetylcholinesterase and the cholinergic neuron. Life Sci 1979;25:1939–1947. [PubMed: 43448]

Lesne S, Koh MT, Kotilnek L, Kayed R, Glabe CG, Yang A, Gallagher M, Ashe KH. A specific amyloid-beta protein assembly in the brain impairs memory. Nature 2006;16:352–357. [PubMed: 16541076]

Levey AI, Wainer BH, Mufson EJ, Mesulam M. Co-localization of acetylcholinesterase and choline acetyltransferase in the rat cerebrum. Neuroscience 1983;9:9–22. [PubMed: 6348584]

Lewis PR, Shute CC. The cholinergic limbic system: projections to hippocampal formation, medial cortex, nuclei of the ascending cholinergic reticular system, and the subfornical organ and supra-optic crest. Brain 1967;90:521–540. [PubMed: 6058141]

Lazarov O, Lee M, Peterson DA, Sisodia SS. Evidence that synaptically released b-amyloid accumulates as extracellular deposits in the hippocampus of transgenic mice. J Neurosci 2002;22:9785–9793. [PubMed: 12427834]

Lüth H-J, Apelt J, Ihunwo AO, Arendt T, Schliebs R. Degeneration of b-amyloid-associated cholinergic structures in transgenic APP_{sw} mice. Brain Res 2003;977:16–22. [PubMed: 12788508]

Lyness SA, Zarow C, Chui HC. Neuron loss in key cholinergic and aminergic nuclei in Alzheimer disease: a meta analysis. Neurobiol Aging 2003;24:1–23. [PubMed: 12493547]

Lysakowski A, Wainer BH, Bruce G, Hersh LB. An atlas of the regional and laminar distribution of choline acetyltransferase immunoreactivity in rat cerebral cortex. Neuroscience 1989;28:291–336. [PubMed: 2646551]

Masters CL, Multhaup G, Simms G, Pottgiesser J, Martins RN, Beyreuther K. Neuronal origin of a cerebral amyloid: neurofibrillary tangles of Alzheimer's disease contain the same protein as the amyloid of plaque cores and blood vessels. EMBO J 1985;4:2757–2763. [PubMed: 4065091]

McLean CA, Cherny RA, Fraser FW, Fuller SJ, Smith MJ, Beyreuther K, Bush AI, Masters CL. Soluble pool of Aβ amyloid as a determinant of severity of neurodegeneration in Alzheimer's disease. Ann Neurol 1999;46:860–866. [PubMed: 10589538]

Mesulam M. The cholinergic lesion of Alzheimer's disease: pivotal factor or side show? Learn Mem 2004;11:43–49. [PubMed: 14747516]

Mesulam M, Mufson EJ, Wainer BH, Levey AI. Central cholinergic pathways in the rat: an overview based on an alternative nomenclature (Ch1-Ch6). Neuroscience 1983;10:1185–1201. [PubMed: 6320048]

Naslund J, Haroutunian V, Mohs R, Davis KL, Davies P, Greengard P, Buxbaum JD. Correlation between elevated levels of amyloid beta-peptide in the brain and cognitive decline. JAMA 2000;283:1571–1577. [PubMed: 10735393]

Oddo S, Caccamo A, Shepherd JD, Murphy MP, Golde TE, Kayed R, Metherate R, Mattson MP, Akbari Y, LaFerla FM. Triple-transgenic model of Alzheimer's disease with plaques and tangles: intracellular A*b* and synaptic dysfunction. Neuron 2003;39:409–421. [PubMed: 12895417]

Oddo S, Caccamo A, Kitazawa M, Tseng BP, LaFerla FM. Amyloid deposition precedes tangle formation in a triple transgenic model of Alzheimer's disease. Neurobiol Aging 2003;24:1063–1070. [PubMed: 14643377]

Oddo S, Vasilevko V, Caccamo A, Kitazawa M, Cribbs DH, LaFerla FM. Reduction of soluble Abeta and tau, but not soluble Abeta alone, ameliorates cognitive decline in transgenic mice with plaques and tangles. J Biol Chem 2006;281:39413–39423. [PubMed: 17056594]

Pakaski M, Kalman J. Interactions between the amyloid and cholinergic mechanisms of Alzheimer's disease. Neurochem Int 2008;53:103–111. [PubMed: 18602955]

Paxinos, G.; Franklin, KBJ. The Mouse Brain in Stereotaxic Coordinates. Elsevier Academic Press; Amsterdam: 2004.

Perez SE, Dar S, Ikonomovic MD, DeKosky ST, Mufson EJ. Cholinergic forebrain degeneration in the APPswe/PS1DE9 transgenic mouse. Neurobiol Dis 2007;28:3–15. [PubMed: 17662610]

Price DL, Sisodia SS. Mutant genes in familial Alzheimer's disease and transgenic models. Ann Rev Neurosci 1998;21:479–505. [PubMed: 9530504]

Rees T, Hammond PI, Soreq H, Younkin S, Brimijoin S. Acetylcholinesterase promotes beta-amyloid plaques in cerebral cortex. Neurobiol Aging 2003;24:777–787. [PubMed: 12927760]

Robertson RT, Baratta J, Yu J, Oddo S, LaFerla FM. Amyloid-beta expression in retrosplenial cortex of triple transgenic mice: relationship to axonal afferents from medial septum. Neurosci Abstr 2007;33:888.6.

Robertson RT, Gallardo KA, Claytor KJ, Ha DH, Ku K-K, Yu BP, Lauterborn JC, Wiley RG, Yu J, Gall CM, Leslie FM. Neonatal treatment with 192 IgG-saporin produces long term forebrain cholinergic

deficits and reduces dendritic branching and spine density of neocortical pyramidal neurons. Cerebral Cortex 1998;8:142–155. [PubMed: 9542893]

Robertson RT, Yu J. Expression of acetylcholinesterase activity in neural development: new tricks for an old dog? News Physiol Sci 1993;8:266–272.

Schenk D, Barbour R, Dunn W, Gordon G, Grajeda H, Guido T, Hu K, Huang J, Johnson-Wood K, Khan K, Kholodenko D, Lee M, Liao Z, Lieberburg I, Motter R, Mutter L, Soriano F, Shopp G, Vasquez N, Vandevert C, Walker S, Wogulis M, Yednock T, Games D, Seubert P. Immunization with amyloid-beta attenuates Alzheimer disease-like pathology in the PDAPPP mouse. Nature 1999;400:173–177. [PubMed: 10408445]

Selkoe DJ. The molecular pathology of Alzheimer's disease. Neuron 1991;6:487–498. [PubMed: 1673054]

Selkoe DJ. Amyloid beta-protein and the genetics of Alzheimer's disease. J Biol Chem 1996;271:18295–18298. [PubMed: 8756120]

Selkoe DJ. Alzheimer's disease is a synaptic failure. Science 2002;298:789–791. [PubMed: 12399581]

Shankar GM, Li S, Mehta TH, Garcia-Munoz A, Shepardson NE, Smith I, Brett FM, Farrell MA, Rowan MJ, Lemere CA, Regan CM, Walsh DM, Sabatini BL, Selkoe DJ. Amyloid-beta protein dimmers isolated directly from Alzheimer's brains impair synaptic plasticity and memory. Nature Medicine 2008;14:837–842.

Sisodia SS, Koo EH, Hoffman PN, Perry G, Price DL. Identification and transport of full-length amyloid precursor proteins in rat peripheral nervous system. J Neurosci 1993;13:3136–3142. [PubMed: 8331390]

Sze CI, Troncoso JC, Kawas C, Mouton P, Price DL, Martin LJ. Loss of the presynaptic vesicle protein synaptophysin in hippocampus correlates with cognitive decline in Alzheimer disease. J Neuropathol Exp Neurol 1997;56:933–944. [PubMed: 9258263]

Takahashi RH, Milner TA, Li F, Nam EE, Edgar MA, Yamaguchi H, Beal MF, Xu H, Greengard P, Gouras GK. Intraneuronal Alzheimer A-beta 42 accumulates in multivesicular bodies and is associated with synaptic pathology. Am J Pathol 2002;161:1869–1879. [PubMed: 12414533]

Tang SJ, Schuman EM. Protein synthesis in the dendrite. Phil Trans R Soc Lond, B 2002;29:521–529. [PubMed: 12028789]

Tengelsen LA, Robertson RT, Yu J. Basal forebrain and anterior thalamic contributions to acetylcholinesterase activity in granular retrosplenial cortex of rats. Brain Res 1992;594:10–18. [PubMed: 1467929]

Terry RD, Masliah E, Salmon DP, Butters N, DeTeresa R, Hill R, Hansen LA, Katzman R. Physical basis of cognitive alterations in Alzheimer's disease: synapse loss is the major correlate of cognitive impairment. Ann Neurol 1991;30:572–580. [PubMed: 1789684]

Van Groen T, Wyss JM. Connections of the retrosplenial granular A cortex in the rat. J Comp Neurol 1990;300:593–606. [PubMed: 2273095]

Vogt BA, Peters A. Form and distribution of neurons in rat cingulate cortex: areas 32, 24, and 29. J Comp Neurol 1981;195:603–625. [PubMed: 7462444]

Wang J, Dickson DW, Trojanowski JQ, Lee VM. The levels of soluble versus insoluble brain Abeta distinguish Alzheimer's disease from normal and pathologic aging. Exp Neurol 1999;158:328–337. [PubMed: 10415140]

Weidemann A, Konig G, Bunke D, Fischer P, Salbaum JM, Masters CL, Beyreuther K. Identification, biogenesis, and localization of precursors of Alzheimer's disease A4 amyloid protein. Cell 1989;57:115–126. [PubMed: 2649245]

Wenk H, Bigl V, Meyer U. Cholinergic projections from magnocellular nuclei of the basal forebrain to cortical areas in rats. Brain Res Rev 1980;2:295–316.

Wilcock DM, Colton CA. Anti-Aβ immunothereapy in Alzheimer's disease; relevance of transgenic mouse studies to clinical trials. J Alz Dis 2008;15:555–569.

Wright CI, Geula C, Mesulam M-M. Neuroglial cholinesterases in the normal brain and in Alzheimer's disease: relationship to plaques, tangles, and patterns of selective vulnerability. Ann Neurol 1993;34:373–384. [PubMed: 8363355]

Yamaguchi H, Nakazato Y, Hirai S, Shoji M, Harigaya Y. Electron micrograph of diffuse plaques. Initial stages of senile plaque formation in the Alzhiemer brain. Am J Pathol 1989;135:593–597. [PubMed: 2679112]

Yazawa H, Yu ZX, Takeda, Le Y, Gong W, Ferrans VJ, Oppenheim JJ, Li CC, Wang JM. Beta amyloid peptide (Abeta42) is internalized via the G-protein coupled receptor FPRL1 and forms fibrillar aggregates in macrophages. FASEBJ 2001;15:2454–2462.

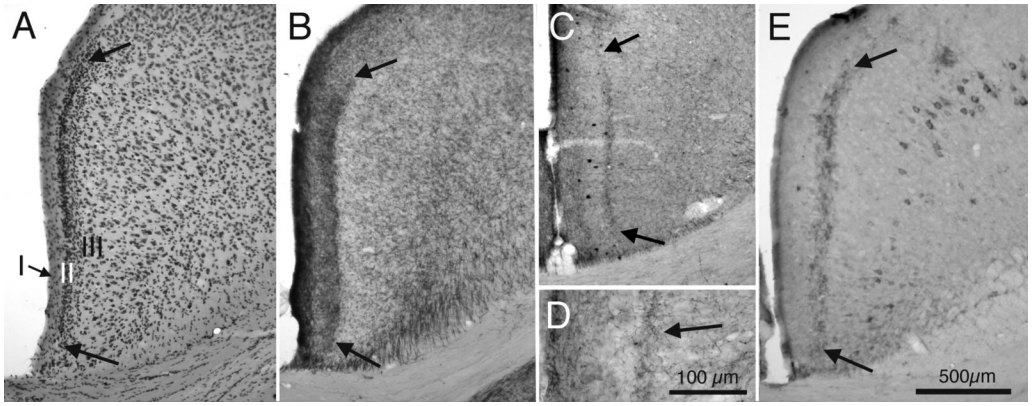

Fig. 1.

Brightfield photomicrographs of transverse sections from granular retrosplenial cortex (RSg) of mice. A: Nissl stained section showing the cytoarchitectural features of RSg of a 3xTg-AD mouse. Cortical layers I, II, and III are indicated; note particularly the dense granular cortical layer II that is characteristic of RSg. Bold arrows indicate the ventral-medial and dorsal-lateral borders of RSg. B: Neighboring section from the same animal processed for AChE histochemistry. Arrows indicate borders of the band of AChE histochemical reaction product in layer III of RSg. C: Comparable section from a different animal, processed for ChAT immunocytochemistry. Arrows indicate the band of ChAT in layer III of RSg. D: Higher magnification photomicrograph of the section shown in 'C', showing axon-like pattern of ChAT immunoreactivity. E: Section adjacent to the section shown in 'B', processed for Aβ immunoreactivity. Arrows indicate the band of A immunoreactivity in layer III; also visible is Aβ immunoreactivity associated with cells in deeper cortical layers. Calibration bar in 'E' = 500μm for Aβ through C and E. Calibration bar in D = 100 μm.

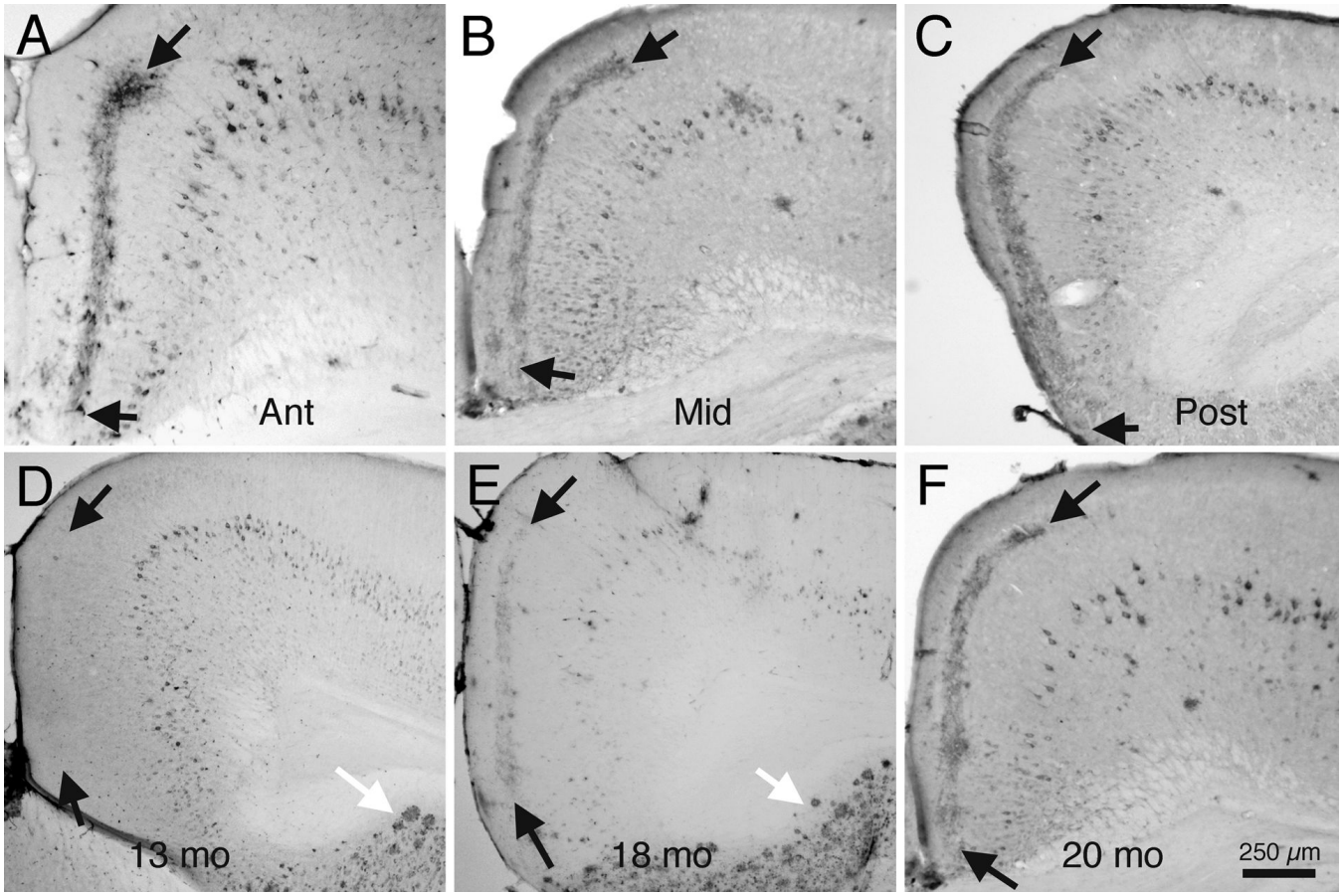

Fig. 2.

Brightfield photomicrographs illustrating patterns of Aβ immunoreactivity in RSg of 3xTg-AD mice. A - C: Transverse sections from a 20 mo old mouse, from anterior portions of RSg (A), through mid-portions (B), to caudal portions (C). Arrows indicate borders of the distinct band of Aβ immunoreactivity in layer III of RSg. D–F: Sections from a developmental series of 3xTg-AD mice, showing onset of Aβ immunoreactivity. D:13 mo old mouse. Note that although many cortical cells display Aβ, and Aβ plaques are seen in the subiculum (white arrow), no Aβ immunoreactivity in visible in layer III of RSg. E: Section from an 18 mo mouse, processed for Aβ. Note the numerous Aβ positive plaques in the subiculum (white arrow), and the light pattern of Aβ immunoreactivity in layer III of RSg (black arrows). F: Section from a 20 mo mouse. Note the dense pattern of Aβ in layer III of RSg. Calibration bar in 'F' = 250 μm for A – F.

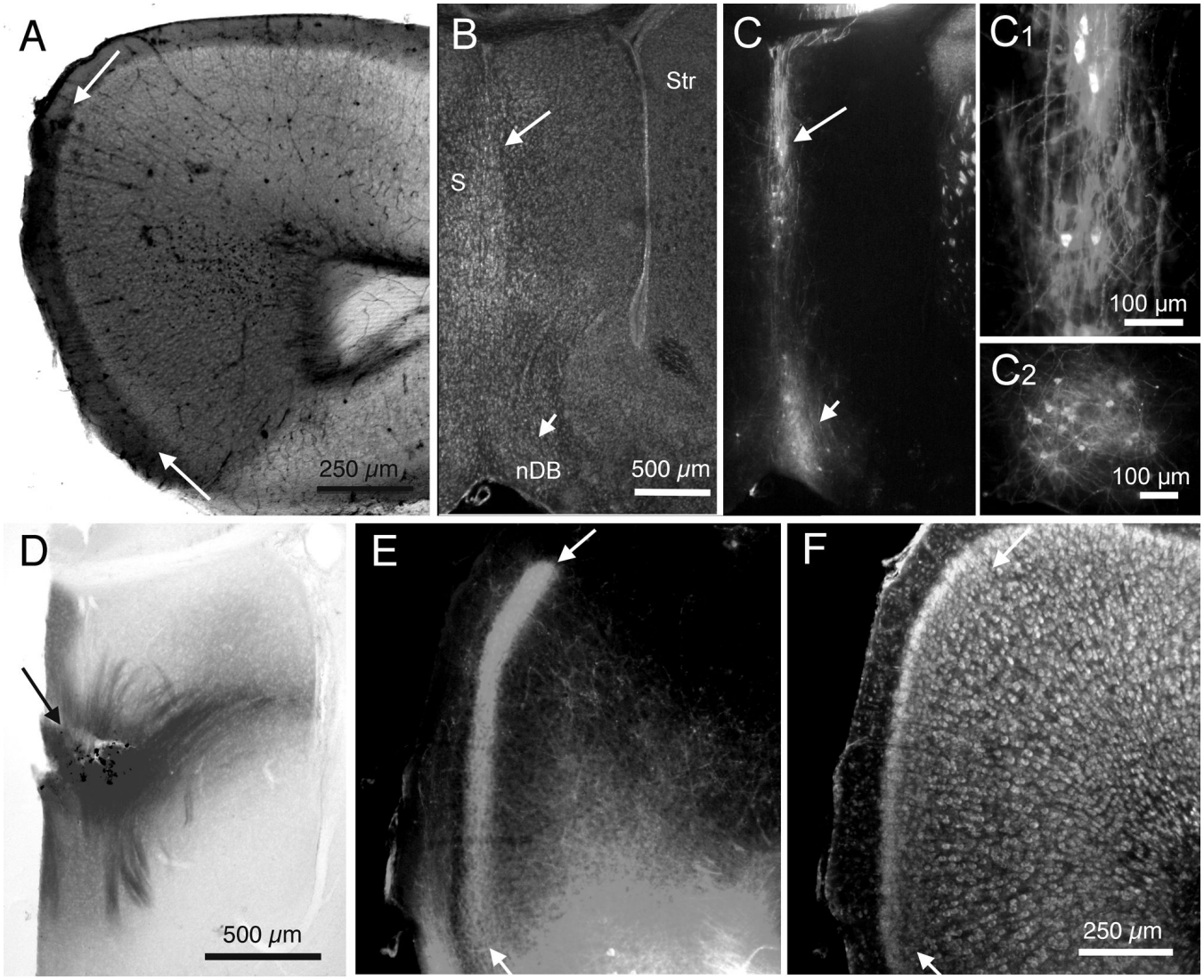

Fig. 3.

DiI tracing of septal projections to RSg in mice. A: Brightfield image of an unstained section showing spread of DiI following a placement in RSg; arrows indicate borders of RSg. B: Fluorescence image of a BoPro labeled section, using fluorescein optics, showing the cytoarchitecture related to DiI labeling in 'C'. C: Fluorescence image, using rhodamine optics, of the same section as in 'B', showing retrograde DiI labeling in septum (long arrow) and nDB (short arrow) in the hemisphere ipsilateral to the DiI placement in A. Arrows indicate same sites shown in 'B'. C1: Higher power photomicrograph of the DiI labeling in medial septum, indicated by the long white arrow in C. C2: Higher power image of DiI labeling of nDB in the section adjacent to the one shown in 'C'. D: Brightfield image of an unstained section showing a DiI placement (arrow) in medial septum. E: Fluorescence image of DiI axonal labeling in layer III of RSg following the DiI placement in D; arrows indicate borders of RSg. F: Fluorescence image of the same section as in 'E', but with fluorescein optics and BoPro staining of cells. Arrows indicate same sites as in 'E'. Calibration bar in 'A' = 250μm. Bar in 'C' = 500 μm for B and C. Bars in C1 and C2 = 100 μm. Bar in 'D' = 500 μm. Bar in 'F' = 250 μm for E and F.

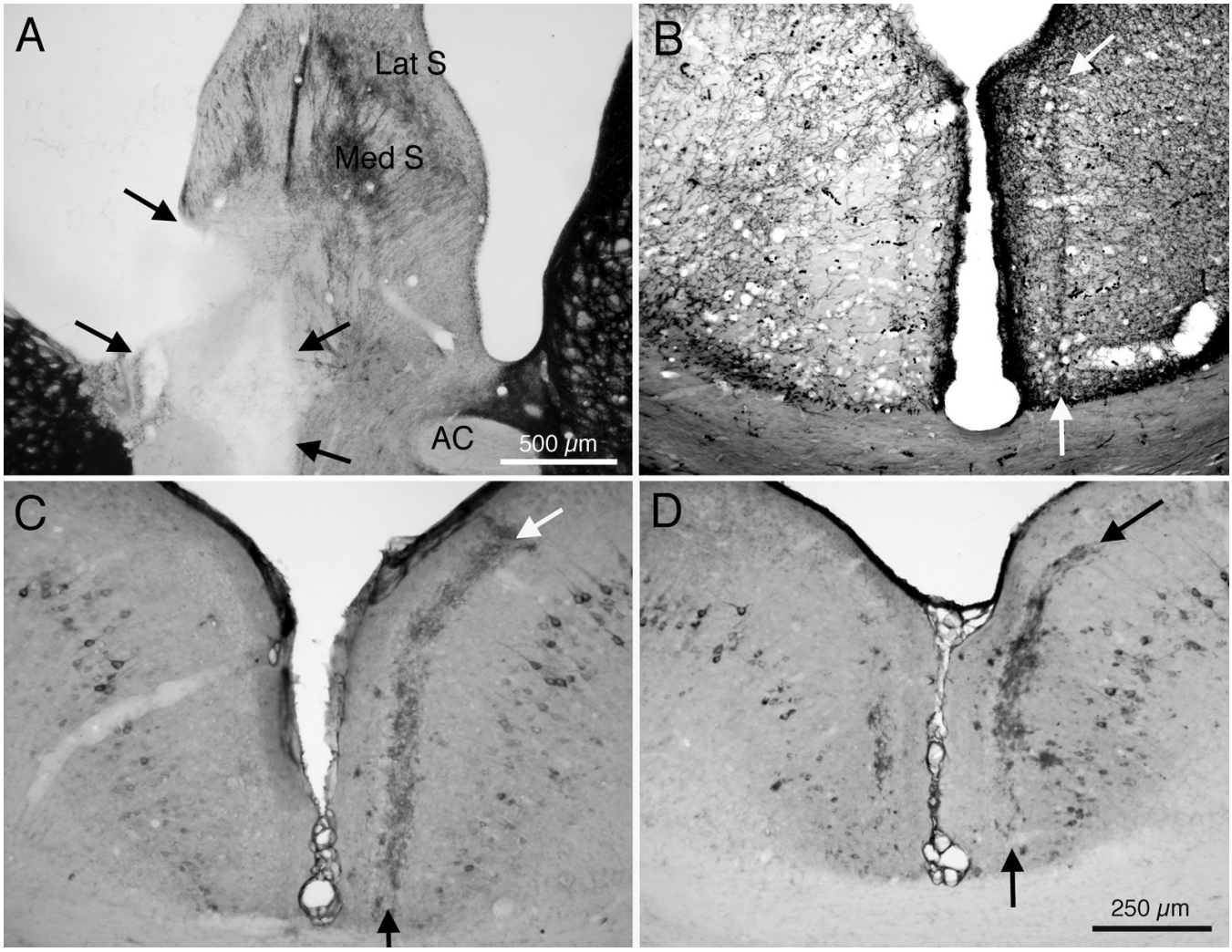

Fig. 4.

Effects of placement of an electrolytic lesion in medial setptum and nDB on Aβ immunoreactivity in RSg of 3xTg-AD mice. A: AChE histochemically stained section though the medial septum; arrows indicate borders of the lesion in the left hemisphere. B: AChE stained section showing loss of AChE activity in RSg of this animal. Arrows indicate borders of AChE positive layer III in the control hemisphere. C: Section showing loss of Aβ immunoreactivity in the left hemisphere of this case. Arrows indicate borders of normal Aβ pattern in the opposite, control hemisphere. D: Section from a different mouse, with a smaller lesion of medial septum, showing partial loss of Aβ immunoreactivity in the left hemisphere. Abbreviations: AC: anterior commisure; Lat S: lateral septum; Med S: medial septum. Calibration bar in A = 500μm; bar in D = 250 μm for B – D.

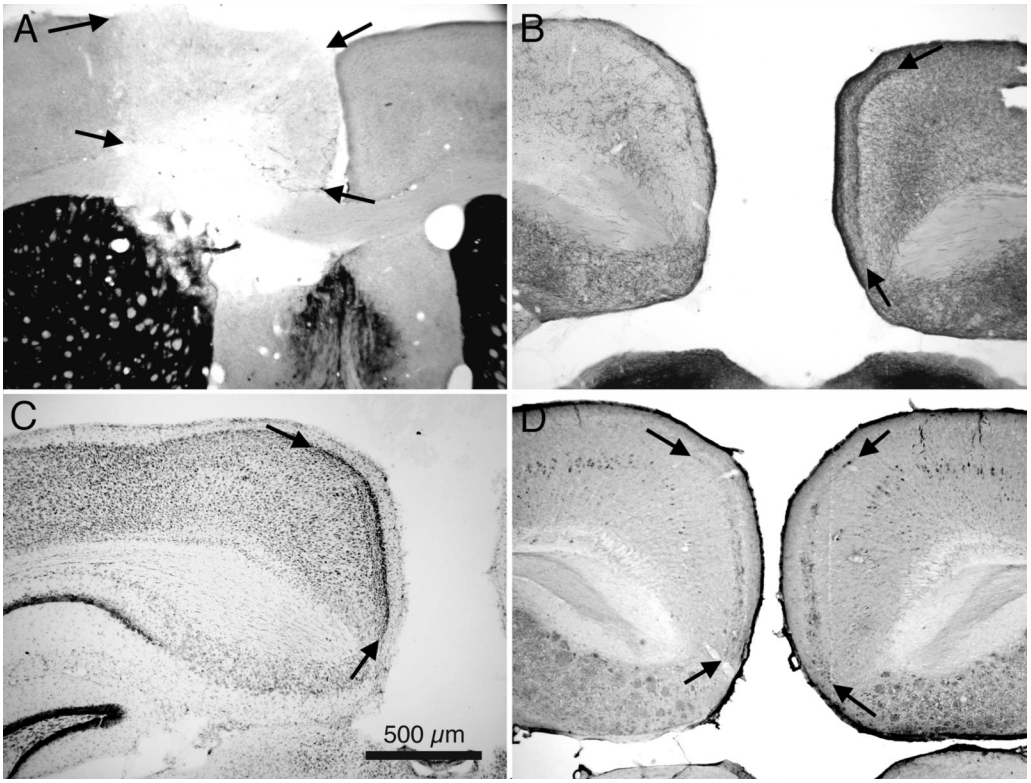

Fig. 5.

Effects of placement of a lesion in the cingulate bundle on Aβ immunoreactivity in RSg of a 3xTg-AD mouse. A: AChE histochemically stained section; arrows indicate borders of the lesion in the cingulate gyrus of the left hemisphere. B: AChE stained section showing loss of AChE activity in RSg of this animal. Arrows indicated borders of the band of AChE in the control hemisphere. C: Section neighboring those in B and D, processed for Nissl to show cytoarchitecture. Arrows indicate borders of the dense layer II that characterizes RSg. D: Section showing only slight loss of Aβ immunoreactivity in the left hemisphere of this case. Arrows indicate borders of the Aβ pattern in the lesioned (left) hemisphere and in the opposite control hemisphere. Calibration bar in C = 500μm; for A – D.

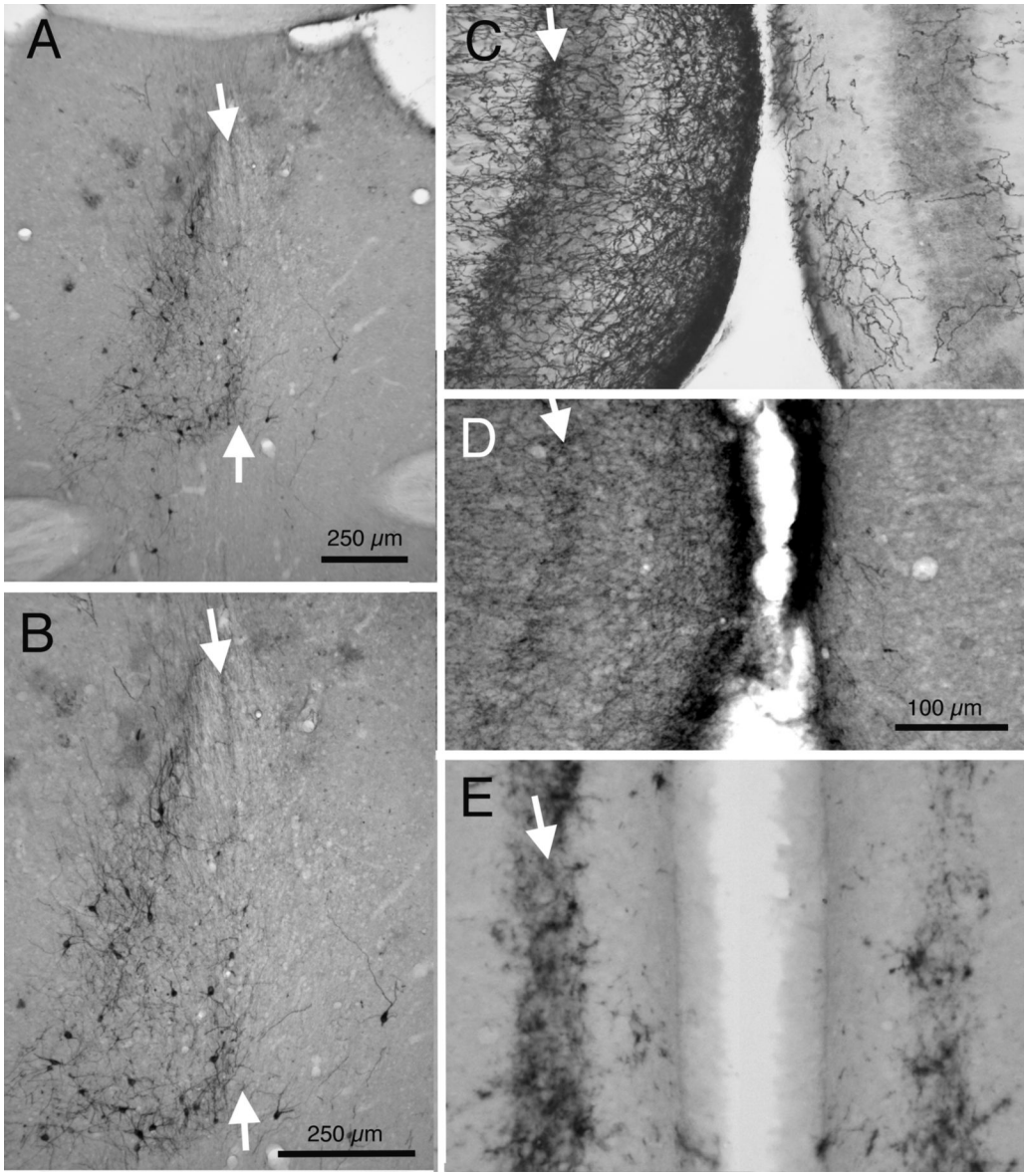

Fig. 6.

Effects of immunolesion of basal forebrain on cholinergic markers and Aβ immunoreactivity in RSg of a 3xTg-AD mouse. A: p75 immunoreactivity in the medial septum; white arrows indicate the midline of the septum. B: Higher power photomicrograph of the section in 'A'; note marked loss of p75 positive cholinergic neurons in the right (lesioned) hemisphere. C: AChE stained section showing loss of AChE activity in the right hemisphere RSg of this animal. Arrow indicates the band of AChE in layer III of the control hemisphere. D: p75 immunoreactivity in a neighboring section to the one shown in 'C'. Note loss of p75 labeled axons in the right (lesioned) hemisphere. E: Neighboring section showing Aβ immunoreactivity; note modest reduction of Aβ in the right hemisphere of this case. Calibration bars in A and B = 250μm; bar in D = 100 μm for C - E.

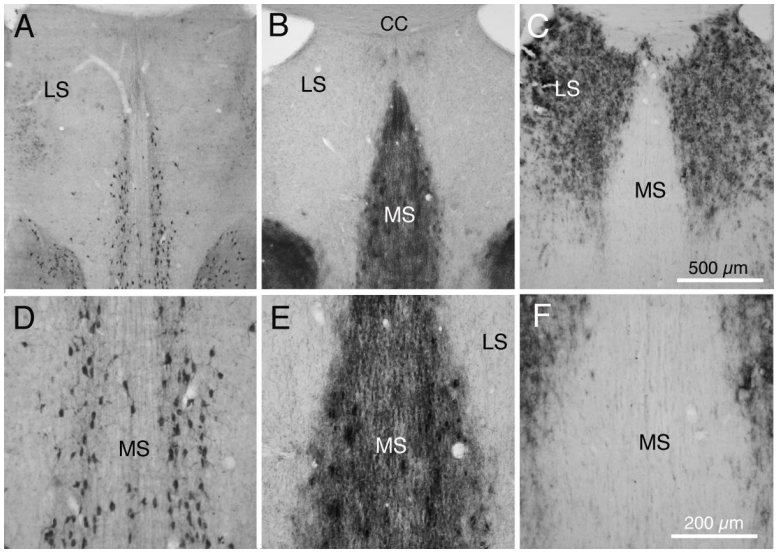

Fig. 7.

Transverse sections from septum of 3xTg-AD mice. A and D: ChAT immunocytochemically processed section from a 23 mo 3XTg-AD mouse, showing ChAT positive neurons in medial septum, but not in lateral septum. B and E: Section from a neighboring section from this mouse, processed for AChE histochemistry; note strong AChE labeling of fibers and some cells in medial septum but only a few fibers in lateral septum. C and F: Section neighboring the section in A, processed for Aβ immunoreactivity, showing dense Aβ plaques in lateral septum, but not in medial septum. Abbreviations: CC: corpus callosum; LS: lateral septum; MS: medial septum. Calibration bar in C = 500 μm for A – C; bar in F = 200 μm for D–F.